Los Alamos Environmental Restoration Records Processing Facility

ER Record I.D.# 49924

LOS ALAMOS

LOS ALAMOS NATIONAL LABORATORY
ENVIRONMENTAL RESTORATION
Records Processing Facility
ER Record Index Form
RPF USE ONLY

PAGE COUNT: 11

DATE RECEIVED: 10/16/95 PROCESSOR: DJC

RECORD CATEGORY (P/R): P INITIALS: DJC

RECORD PACKAGE NO.: —

FILE FOLDER: —

CORRECTION (Y/N): — CORRECTED NO.: — CORRECTED BY: —

AR (Y/N): yes INITIALS: DJC

AR DESCRIPTION (D/G): —

PRIVILEGED Y/N: —

ELECTRONIC INDEX INITIALS: DJC

MISCELLANEOUS: OU 1098

This form is subject to change

14007

indfrm 01/18/95

GARDNER

~~Fraser Gu~~

w/ notations

(11)

EARTH AND PLANETARY SCIENCE LETTERS 2 (1967) 163-173. NORTH-HOLLAND PUBL. COMP., AMSTERDAM

Geol. Soc. Amer.
...lvania State Un...
...r. (1966) 166
. Geol. Soc. Amer.
Geochim. Cosm...
63) 533.
530.
...eol. 74 (1966) 197.
...eol. 74 (1966) 217.

PLIOCENE GEOMAGNETIC POLARITY EPOCHS *

G. B. DALRYMPLE, Allan COX, Richard R. DOELL and C. S. GROMMÉ
U.S. Geological Survey, Menlo Park, California, USA

Received 17 March 1967

A paleomagnetic and K-Ar dating study of 44 upper Miocene and Pliocene volcanic units from the western United States suggests that the frequency of reversals of the earth's magnetic field during Pliocene time may have been comparable with that of the last 3.6 m.y. Although the data are too limited to permit the formal naming of any new polarity epochs or events, four polarity transitions have been identified: the W10 R/N boundary at 3.7 ± 0.1 m.y., the A12 N/R boundary at 4.9 ± 0.1 m.y., the W32 N/R boundary at 9.0 ± 0.2 m.y., and the W36 R/N boundary at 10.8 ± 0.3 - 1.0 m.y. The loss of absolute resolution of K-Ar dating in older rocks indicates that the use of well defined stratigraphic successions to identify and date polarity transitions will be important in the study of Pliocene and older reversals.

1. INTRODUCTION

Recent paleomagnetic and potassium-argon dating research on upper Cenozoic volcanic rocks from the United States, Europe, Africa and Réunion has led to the development of a time scale of reversals of the earth's magnetic field for the past 3.6 m.y. [1-4]. This geomagnetic polarity time scale consists of a series of four epochs, which are periods of time during which the magnetic field was predominantly or entirely of one polarity, and three events, which are like epochs but are about an order of magnitude shorter in duration.

Besides conclusively demonstrating that the earth's magnetic field has undergone frequent and irregularly spaced reversals of polarity in late Cenozoic time, the polarity time scale provides a distinctive and world wide sequence of sharply defined time horizons that can be used as an aid to correlation and age assignment in stratigraphic studies. The recent discovery of a reversal stratigraphy in deep-sea sediment cores [5, 6] has broadened the applicability of the reversal time scale to oceanographic research, and geomagnetic reversals provide vital evidence for the Vine-Matthews theory of the ocean floor spreading outward from mid-oceanic ridges [7, 8].

In view of the usefulness of the present reversal time scale to both geophysics and to stratigraphy, it seems worthwhile to attempt to extend it beyond 3.6 m.y. ago. During the past year our research on reversals has been directed toward gathering data on the frequency and timing of geomagnetic reversals during upper Miocene and Pliocene time. In this paper, we present the results of combined paleomagnetic-geochronometric studies of 44 volcanic units from the western United States that range in age from about 2-16 m.y.

Potassium-argon dating was done by standard isotope dilution techniques using a bulb tracer system and a Reynolds-type mass spectrometer for mass analyses. Potassium determinations were made by flame photometry using a lithium internal standard. Our criteria for selecting suitable samples for whole-rock analyses are explained by Cox et al. [4]. Details of the analytical procedures and the results of our analyses of interlaboratory standards are described by Lanphere and Dalrymple [9].

The paleomagnetic sampling can be classified into two of the magnetic categories defined by Cox et al. [4]. For 36 of the units studied, multiple oriented cores were measured in the laboratory and magnetic stability tests were made on at least 1 core (category IIIA). For 8 units, polarity determinations were made on multiple hand samples in the field with a portable fluxgate magnetometer [10], and cores from at least one of the hand samples were checked in the laboratory for both polarity and magnetic stability (category IIIB). The laboratory magnetic measurements and a.c. demagnetization experiments were done using equipment and techniques described by Doell and Cox [11, 12].

*Publication authorized by the Director, U.S. Geological Survey.

Received by ER-RPF
OCT 16 1995
Dic

Table 1
Analytical data for potassium-argon age determinations.

Sample	Material analyzed	K_2O (wt. %)	Argon: Sample weight (g)	Argon: $^{40}Ar_{rad}$/g (10^{-11} moles)	Argon: $^{40}Ar_{rad} \times 100 / {}^{40}Ar_{total}$	$^{40}Ar_{rad} / {}^{40}K$ (10^{-4})	Calculated age * (10^6 y)
New Mexico							
W1 - Qtz. latite of Santa Clara Canyon	plagioclase	0.321, 0.321, 0.335	2.040 4.911	0.256 0.255	6.1 10.4	3.222	5.50 ± 0.82
W2 - Andesite of Santa Clara Canyon	plagioclase	0.823, 0.811	3.180	0.897	29.2	3.909	6.69 ± 0.33
W3 - Basalt of Polvadera Mesa	basalt	1.26, 1.27	10.433 12.410	1.387 1.357	60.9 72.7	4.356	7.43 ± 0.16
W4 - Qtz. latite near Polvadera Sawmill	plagioclase	0.751, 0.757	8.102 8.356	4.697 4.544	40.3 54.2	2.943	5.03 ± 0.13
W5 - Rhyolite near El Rechuelos	obsidian	4.55, 4.55 4.55, 4.60	4.202 4.995	1.370 1.364	27.6 36.5	1.184	2.02 ± 0.06
W6 - Rhyodacite of Cañada del Ojitos	plagioclase	0.620, 0.616	7.315 11.430	0.610 0.605	33.9 49.1	3.892	6.64 ± 0.17
	biotite	5.03, 6.23 6.15, 6.09	3.399	2.857	15.0	1.845	3.15 ± 0.28
W7 - Dacite of Bland Canyon	plagioclase	0.666, 0.669	5.654 8.508	0.574 0.879	40.7 47.2	5.198	8.87 ± 0.19
W8 - Rhyodacite near Rancho Cañada	plagioclase	0.640, 0.642	10.264 10.676	0.864 0.862	49.6 48.0	5.332	9.09 ± 0.19
W9 - Andesite of St. Peters Dome	plagioclase	0.655, 0.657 0.690, 0.694	10.304 10.126	0.850 0.849	35.3 34.0	4.962	8.46 ± 0.38
W10 - Rhyodacite of Cerro Grande	plagioclase	0.474, 0.474	11.139 10.791	0.255 0.260	24.2 28.1	2.150	3.67 ± 0.32
W11 - Rhyodacite near Abiquiu Creek	plagioclase	0.577, 0.575	9.437 9.065	0.478 0.482	27.6 27.3	3.300	5.63 ± 0.18
W12 - Perlite of Grants Mesa	sanidine	10.50, 10.99	5.252	4.413	60.9	1.603	2.74 ± 0.08
Oregon							
W13 - Basalt near Crooked Creek	basalt basalt	0.373, 0.375 0.371, 0.374	9.769 11.652	0.436 0.431	16.0 15.6	4.611 4.576	7.87 ± 0.55 7.81 ± 0.55
W14 - Lower tuff of Rattlesnake Formation	anorthoclase	5.00, 4.95	0.675	4.923	39.6	3.913	6.69 ± 0.20
W15 - Upper tuff of Rattlesnake Formation	anorthoclase	5.69, 5.67	1.027	4.998	47.9	3.484	5.95 ± 0.18
W16 - Welded tuff of Drewsey Formation of Bowen et al. in [20]	sanidine	7.26, 7.24	2.788 2.570	9.690 9.763	81.3 81.1	5.366	9.15 ± 0.19
W17 - Rhyolite tuff near Twelve Mile Creek	sanidine	7.18, 7.36	1.569 1.569	17.09 17.03	80.0 83.7	9.288	15.81 ± 0.40
W18 - Rhyolite tuff near Battle Creek	sanidine	[illegible]	[illegible]	[illegible]	[illegible]	[illegible]	[illegible]

Table 1 (continued)

Sample	Material analyzed	K_2O (wt. %)	Argon: Sample weight (g)	Argon: $^{40}Ar_{rad}$/g (10^{-11} moles)	Argon: $^{40}Ar_{rad} \times 100 / {}^{40}Ar_{total}$	$^{40}Ar_{rad} / {}^{40}K$ (10^{-4})	Calculated age * (10^6 y)
Nevada							
[illegible]	sanidine	10.51, 10.49	8.138	5.156	91.6	1.844	3.32 ± 0.10

W18 - Upper tuff of Rattlesnake Formation	sanidine	7.26 , 7.24	2.788 2.570	9.890 9.763	81.3 81.1	3.388	9.15 ± 0.19
W16 - Welded tuff of Drawsey Formation of Bowen et al. in [20]	sanidine	7.19 , 7.36	1.569 1.569	12.09 12.05	80.0 83.7	9.288	15.81 ± 0.40
W17 - Rhyolite tuff near Twelve Mile Creek	sanidine	8.51 , 8.62	1.209 1.194	17.49 14.95	79.2 77.8	7.940	13.56 ± 0.29
W18 - Rhyolite tuff near Battle Creek	sanidine						

Table 1 (continued)

Sample	Material analyzed	K_2O (wt. %)	Argon: Sample weight (g)	Argon: $^{40}Ar_{rad}$/g (10^{-11} moles)	Argon: $\frac{^{40}Ar_{rad} \times 100}{^{40}Ar_{total}}$	$\frac{^{40}Ar_{rad}}{^{40}K}$ (10^{-4})	Calculated age * (10^6 y)
Nevada							
W19 - Perlite near Anchorite Pass, sample no. 1	sanidine	10.51 , 10.43	8.138	5.156	91.6	1.944	3.32 ± 0.10
	biotite	7.35 , 7.39	4.430	3.695	23.0	1.953	3.39 ± 0.24
W19 - Perlite near Anchorite Pass, sample no. 2	sanidine	10.59 , 10.52	8.510	4.976	50.1	1.866	3.19 ± 0.10
	biotite	7.70 , 7.76	3.952	3.939	25.7	2.017	3.45 ± 0.17
W20 - Biotite andesite near Anchorite Pass	biotite	8.18 , 8.21	3.840	4.190	32.6	2.024	3.46 ± 0.14
	plagioclase	0.669, 0.671	7.654	0.373	17.9	2.206	3.77 ± 0.34
W21 - Basalt near Anchorite Pass	basalt	1.83 , 1.83	11.261 11.067	0.945 0.946	29.2 29.3	2.050	3.50 ± 0.11
W22 - Lousetown Formation	basalt	0.945, 0.964 0.961, 0.932	10.605 11.505	0.960 0.993	66.7 61.4	4.043	6.90 ± 0.15
California							
W23 - Biotite-augite latite tuff near Anchorite Pass	biotite	7.97 , 8.04	1.692	11.28	59.9	5.599	9.52 ± 0.36
W24 - Biotite-augite latite tuff north of Mono Lake	biotite	7.58 , 8.02	2.659	10.89	69.5	5.389	9.19 ± 0.28
W25 - Biotite-augite latite tuff near Conway Summit, sample no. 1	biotite	7.91 , 7.92	2.039	10.96	63.7	5.493	9.35 ± 0.37
W25 - Biotite-augite latite tuff near Conway Summit, sample no. 2	biotite	7.81 , 7.86	3.055	10.46	73.4	5.283	9.01 ± 0.27
W26 - Alturas Formation of Dorf [23], welded tuff	plagioclase	0.496, 0.501	6.780 7.549	0.983 0.977	29.0 35.4	7.782	13.26 ± 0.33
W27 - Hornblende andesite intrusion near Blairsden	plagioclase	0.173, 0.174	6.972	0.218	16.0	6.335	10.81 ± 0.54
W28 - Hypersthene basalt of Stony Ridge	basalt	0.559, 0.563	11.359	1.141	72.0	8.064	13.74 ± 0.41
W29 - Latite of Bald Peak	basalt basalt	1.99 , 2.00 1.72 , 1.72	12.079 14.576	2.592 2.374	29.4 26.5	5.845 5.459	8.78† ± 0.40 9.31 ± 0.42
Alaska							
Basalts of Nunivak Island							
A1	basalt	1.51 , 1.53	10.341	1.377	54.9	3.596	6.12 ± 0.18
A2	basalt	1.08 , 1.09	10.502	0.664	44.7	2.422	4.14 ± 0.12
A3	basalt	0.573, 0.577	10.568	0.592	42.3	2.363	4.04 ± 0.12
A9	basalt	0.996, 0.996	10.188	0.713	46.8	2.834	4.84 ± 0.15
A11	basalt	1.03 , 1.04	10.284	0.748	52.0	2.859	4.89 ± 0.15
A12	basalt	1.04 , 1.04	10.777	0.743	49.8	2.827	4.83 ± 0.14
A15	basalt	1.70 , 1.71	11.437	1.278	61.1	2.968	5.05 ± 0.15
A17	basalt	1.37 , 1.35	11.216	0.992	53.3	2.857	4.88 ± 0.15

* $\lambda_\epsilon = 0.585 \times 10^{-10}\ y^{-1}$, $\lambda_\beta = 4.72 \times 10^{-10}\ y^{-1}$, $^{40}K/K_{total} = 1.19 \times 10^{-4}$ mole/mole. The (±) figures are estimates of the precision at the 68% confidence level and were calculated using the method described by Cox and Dalrymple [13].
† Recalculated from data given in [21].

Table 2

Summary of Pliocene radiometric and magnetic data for the western United States. Data in parentheses are assigned to the secondary group and are not considered reliable for defining the polarity time scale for reasons discussed in the text. N = normal polarity. R = reversed polarity. magnetic categories are explained in the text.

Unit name	No.	K-Ar age 10^6 y	Polarity	Magnetic category
Rhyolite near El Rechuelos	W5	2.02 ± 0.06	R	III A
Perlite of Granite Mesa	W12	3.74 ± 0.08	N	III A
Perlite near Anchorite Pass	W19	3.34 ± 0.11	R	III A
Basalt near Anchorite Pass	W21	3.50 ± 0.11	R	III A
Biotite andesite near Anchorite Pass	W20	3.82 ± 0.18	R	III A
Rhyodacite of Cerro Grande	W10	3.87 ± 0.12	N	III A
Basalt of Nunivak Island	A3	4.04 ± 0.12	N	III B
Basalt of Nunivak Island	A2	4.14 ± 0.12	N	III B
Rhyolite of Nobel Canyon	W30	4.75 ± 0.07 *	R	III A
Basalt of Nunivak Island	A12	4.83 ± 0.14	N	III B
Basalt of Nunivak Island	A8	4.84 ± 0.15	R	III B
Basalt of Nunivak Island	A11	4.88 ± 0.15	R	III B
Basalt of Nunivak Island	A17	4.88 ± 0.15	N	III B
Qtz. latite near Polvadera Sawmill	W4	5.03 ± 0.13	N	III A
Basalt of Nunivak Island	A15	5.06 ± 0.15	N	III B
(Qtz. latite of Santa Clara Canyon)	(W1)	(5.50 ± 0.82)	(N)	(III A)
Rhyodacite near Ahiquin Creek	W11	5.63 ± 0.18	N	III A
Rattlesnake Formation, upper unit	W15	5.95 ± 0.18	R	III A
Basalt of Nunivak Island	A1	6.12 ± 0.18	N	III B
Rhyodacite of Cañada del Ojitos	W6	6.64 ± 0.17	N	III A
Rattlesnake Formation, lower unit	W14	6.69 ± 0.20	R	III A
Andesite of Santa Clara Canyon	W2	6.69 ± 0.33	N	III A
Louselown Formation	W22	6.90 ± 0.19	R	III A
Basalt of Boreal Ridge	W31	7.4 ± 0.2 *	N	III A
Basalt of Polvadera Mesa	W3	7.43 ± 0.16	N	III A
Basalt near Crooked Creek	W13	7.84 ± 0.34	R	III A
Andesite of St. Peters Dome	W9	8.46 ± 0.38	N	III A
Biotite-augite latite tuff of Bald Peak	W32	8.8 ± 0.2 **	R	III A
Dacite of Bland Canyon	W7	8.87 ± 0.19	R	III A
Latite of Table Mountain	W33	9.0 ± 0.2 *	R	III A
Latite of Bald Peak	W29	9.04 ± 0.29	N	III A
Rhyodacite near Rancho Cañada	W8	9.09 ± 0.19	N	III A
Welded tuff of Drewsey Formation of Bowen et al., in [20]	W16	9.15 ± 0.19	N	III A
Biotite-augite latite tuff near Conway Summit	W25	9.18 ± 0.22	N	III A
Biotite-augite latite tuff north of Mono Lake	W24	9.19 ± 0.28	R	III A
Biotite-augite latite tuff near Anchorite Pass	W23	9.52 ± 0.38	R	III A
Basalt of Coyote Flat	W34	9.6 ± 0.2 **	R	III A
(Basalt of Deep Springs Valley)	(W35)	(10.8 ± 1.0 **)	(R)	(III A)
Hornblende andesite intrusion near Blairsden	W27	10.81 ± 0.54	N	III A
Rhyolite tuff of Deep Springs Valley	W36	10.9 ± 0.2 **	N	III A
Welded tuff of Alturas Formation of Dorf [28]	W26	13.26 ± 0.33	N	III A
Rhyolite tuff near Battle Creek	W18	13.56 ± 0.28	N	III A
Hypersthene basalt of Stony Ridge	W28	13.74 ± 0.41	N	III A
Rhyolite tuff near Twelve Mile Creek	W17	15.81 ± 0.40	N	III A

* Ref. [21].
** Ref. [22].

2. RESULTS

The analytical data for K-Ar ages are presented in table 1. For each determination, an estimate of the standard deviation of precision was made using the method described by Cox and Dalrymple [13]. Where multiple determinations were made, the results were averaged and the precision estimates were compounded by standard statistical techniques [14].

The calculated ages and magnetic polarities of all but one of the units (table 2) are compatible with the known stratigraphic and geochronometric data, details of which are given in the appendix. For sample W6, the biotite gave a considerably younger age (3.15 m.y.) than the two plagio-

clase determinations. (E
amination of the biotite
not show any significant
biotite pattern, but
that the biotite has bee
and that the iron in
During the argon extrac
sually large amount of
the mineral. Thin sec
rock indicates that the
occurred at the time of
due to weathering. Appa
alteration was suffic
We therefore consider
plagioclase to be the t
age of sample W6.

In our previous wor
venient to divide the p
data into a primary dat
suitably reliable, for
scale, and a less relia
13]. Primary data are
lowing criteria: 1) the
include laboratory test
ty; 2) the estimated st
sion of the K-Ar ages
0.1 m.y. or 5.0%, wh
magnetic and age me

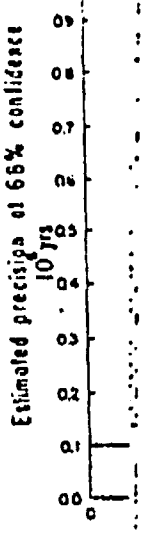

Fig. 1. Precision of the
ity data. The solid line
signed to the

-lase determinations (6.64 m.y.). An X-ray examination of the biotite with a diffractometer did show any significant departure from a normal biotite pattern, but optical examination suggests that the biotite has been oxidized and hydrated and that the iron is mostly in the ferric state. During the argon extraction experiment, an unusually large amount of water was released from the mineral. Thin section examination of the rock indicates that the oxidation and hydration occurred at the time of crystallization and is not due to weathering. Apparently, this slight deuteric alteration was sufficient to cause argon loss. We therefore consider the calculated age of the plagioclase to be the best approximation of the age of sample W6.

In our previous work, we have found it convenient to divide the paleomagnetic-radiometric data into a primary data set, which includes data suitably reliable for defining a polarity time scale, and a less reliable secondary data set [1, 13]. Primary data are those that satisfy the following criteria: 1) the magnetic measurements include laboratory tests for polarity and stability; 2) the estimated standard deviation of precision of the K-Ar ages is less than or equal to 0.1 m.y. or 5.0%, whichever is larger; 3) the magnetic and age measurements were made on the same or on time-equivalent cooling units; and 4) the determinations were made on reliable material. Although data in the secondary group are satisfactory for many geologic purposes and can provide useful information relating to the polarity epoch time scale, it is our opinion that they are not reliable enough to be used in the formal naming of epochs or events.

The data in table 2 satisfy the criteria for primary classification except for units W1 and W35, which are assigned to the secondary group on the basis of the large uncertainties in the K-Ar age determinations (fig. 1).

Primary and secondary data are plotted against time in fig. 2, which also shows the reversal time scale for the last 3.6 m.y. Where the new data overlap the previously determined time scale, they are in agreement with it. Probably the most striking feature of the plot is that no obvious pattern of reversals is readily apparent. In view of the limited number of data, this is not surprising, because the percentage error in K-Ar dating varies around a more or less constant value, whereas the absolute dating error increases with age. If the frequency of reversals during Pliocene time was similar to that of the last 3.6 m.y. (approximately 2.5 polarity transitions per m.y.), then for the early and middle

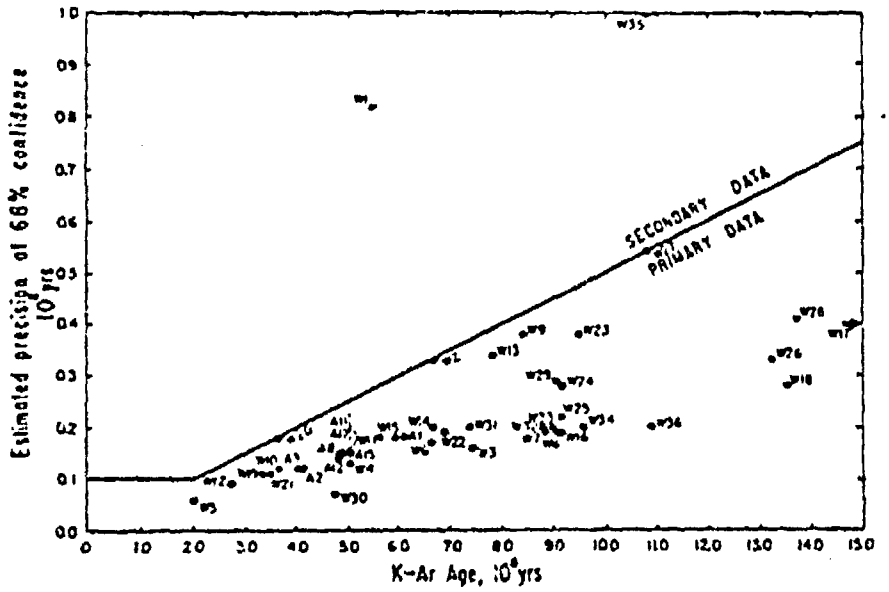

Fig. 1. Precision of the K-Ar age determinations (68% confidence level) versus age for the 44 upper Cenozoic polarity data. The solid line represents 0.1 m.y. or 5.0% of the age, whichever is greater. Data above the line are assigned to the secondary group and are not considered reliable for defining the polarity time scale.

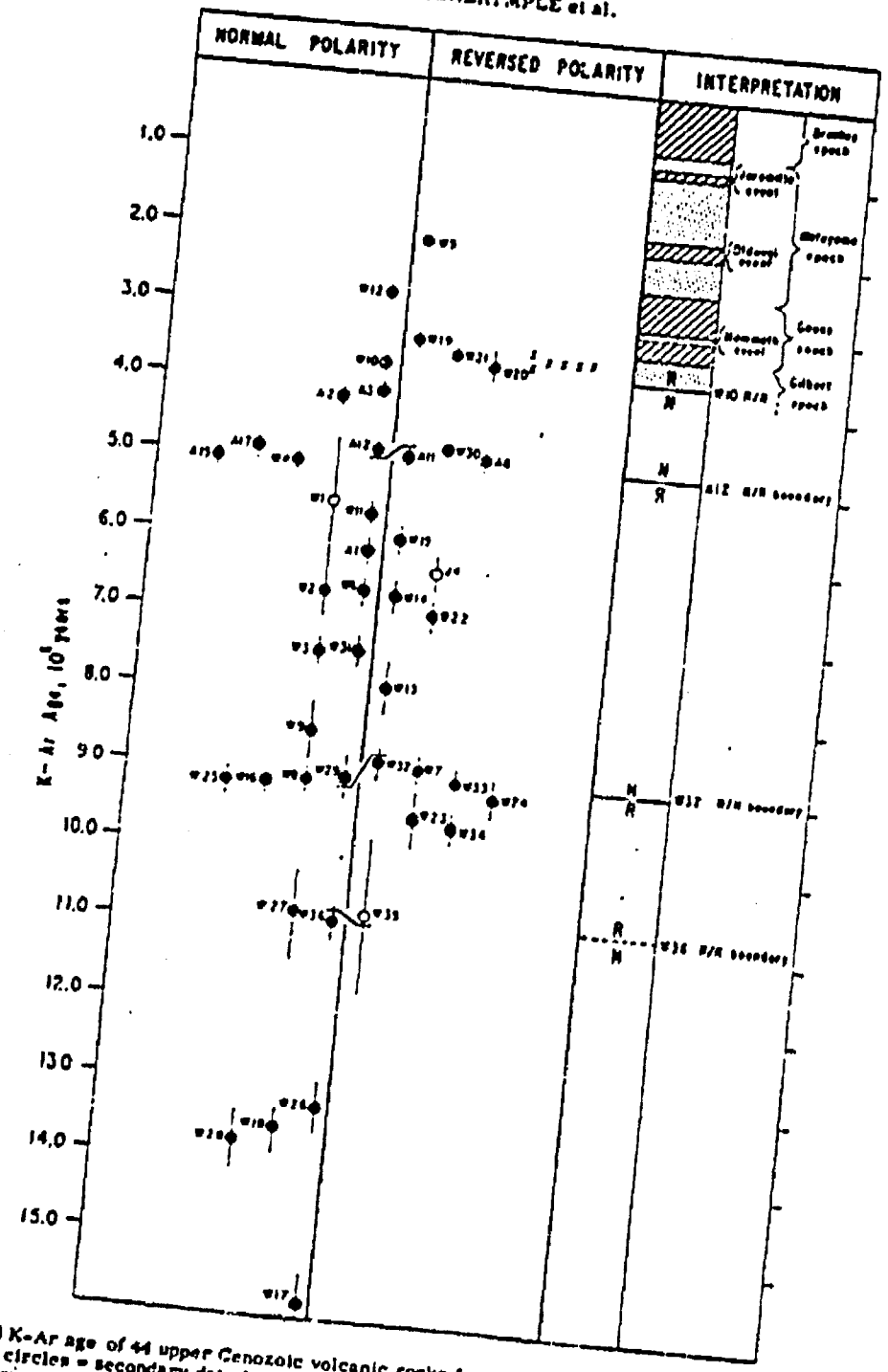

olarity and K-Ar age of 44 upper Cenozoic volcanic rocks from the western United States. Shaded circles = ata, open circles = secondary data (see text), x = previously published data for the Gilbert epoch [1]. The ars are the estimated precision of the K-Ar ages at the 68% confidence level. The horizontal bars indicate position relationships between flows of opposite polarity. The previously determined polarity time scale erval from 0 to 3.6 m.y. ago [1-4] is shaded with hatched pattern for normal polarity and dotted pattern for reversed polarity.

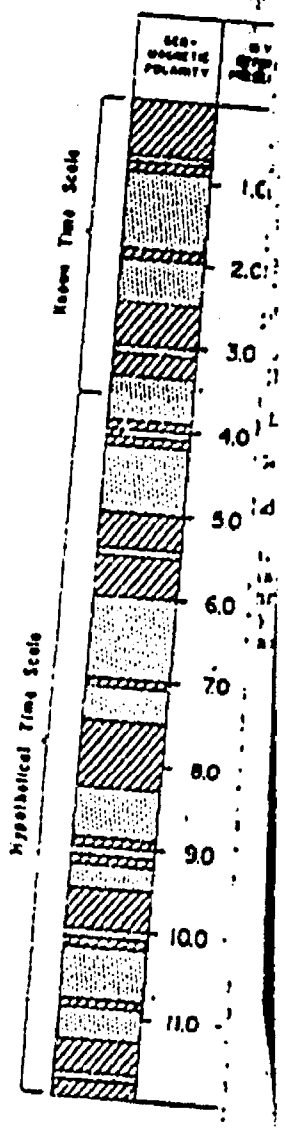

Fig. 3. Percentage of samples l polarity as a function of their dating precision of ±3.0% (sta infinite sample density. The l the assumed polarity of the geo = normal, dotted = reversed). prior to 3.6 m.y. are entirely l tended only to show the loss K-Ar dating for the earlier pa scale. The curve was calculate model described by Cox an

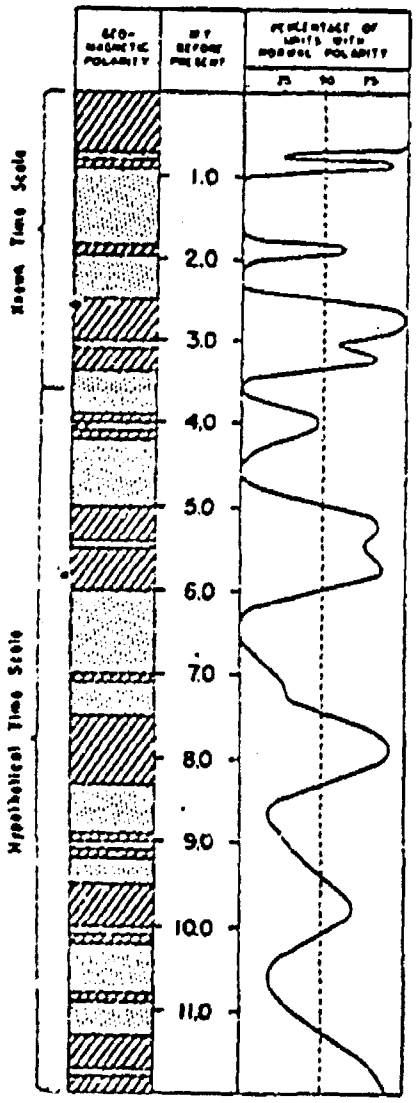

Fig. 3. Percentage of samples that would have normal polarity as a function of their K-Ar ages, assuming a dating precision of ±3.0% (standard deviation) and an infinite sample density. The left-hand column shows the assumed polarity of the geomagnetic field (hatched = normal, dotted = reversed). The assumed polarities prior to 3.6 m.y. are entirely hypothetical and are intended only to show the loss of resolving power of K-Ar dating for the earlier part of the reversal time scale. The curve was calculated using the probability model described by Cox and Dalrymple [13].

Pliocene the dating errors will be large relative to the lengths of polarity epochs and much larger than the average event length. Thus even the major features of the middle and early Pliocene reversal time scale are difficult to resolve.

This difficulty in working with pre-Pleistocene polarity data has been predicted by Cox and Dalrymple on the basis of theoretical considerations [13]. Fig. 3 shows the percentage of normal units to be expected as a function of their age, assuming that the earth's magnetic field has changed polarity as shown at the left-hand side of the diagram (polarity transitions older than 3.6 m.y. ago are hypothetical). The curve was calculated using a standard deviation of precision of 3.0% for the dating and is based on an infinite sample density throughout the entire age range. It is apparent from the figure that polarity events will probably not be distinguishable from dating errors in rocks older than about 6 m.y. If the random sampling techniques that were successful for defining the sequence of reversals for the last 3.6 m.y., are used, even major Pliocene polarity epochs will be difficult to define without an immense amount of data.

The only readily distinguishable features of the Pliocene reversal time scale are four epoch or event boundaries. Of these, three are recognizable only because the relationship between dated normal and reversed rocks could be determined directly by stratigraphic superposition. Thus, it appears that boundaries, especially when represented by superposed units, will be identifiable and useful before epochs and events, and that the use of well defined stratigraphic successions will be increasingly important in the study of Pliocene reversals.

For ease of identification and reference, we have given the four recognizable boundaries temporary designations. Each boundary is identified by the number of one of the relevant samples along with the sense of the transition, i.e.,

Table 3
Identifiable Pliocene polarity boundaries and their approximate potassium-argon ages. The (±) figures are estimates of the uncertainties in boundary age assignments at the two-thirds confidence level.

Boundary designation	K-Ar age (10^6 y)
W10 R/N	3.7 ± 0.1
A12 N/R	4.9 ± 0.1
W32 N/R	9.0 ± 0.2
	+ 0.3
W36 R/N	10.8
	− 1.0

aded circles = epoch [1]. The bars indicate ity time scale ed pattern for

N/R for normal stratigraphical over reversed. In addition, an estimated confidence limit has been assigned to the age of each boundary (table 3). The ages of three of the boundaries can be assigned quite closely, but the upper limit of the fourth, the W36 R/N boundary, is somewhat uncertain because the overlying reversed rock (W35) is a secondary datum. In any case, the boundary must be older than the age of the reversed points W33 and W34.

With the exception of the four boundaries listed in table 3, a number of equally plausible interpretations are compatible with the remaining Pliocene data if the 95% confidence limits of the age determinations are considered. The only definite statement that can be made at this time is that a minimum of three additional polarity transitions must exist between the A12 N/R and the W32 N/R boundaries. It does not seem worthwhile to speculate beyond this until additional data are available.

APPENDIX

Following are sample locations, the lateral span of paleomagnetic samples, and pertinent geologic information. Unless otherwise noted, the dated sample unit is either the same as the paleomagnetic samples or was collected at the same locality. With the exception of W3, which is a basalt flow, units W1-W11 are volcanic domes that were emplaced prior to the formation of the Valles Caldera in New Mexico [15]. Unit W5 is thought to be the youngest. The remaining domes can be divided geologically into two groups, within which the stratigraphic relationships cannot be determined. Units W7-W9 form the older group and units W1, W2, W4, W6, W10 and W11 the younger group [16].

1. Guaje Mountain, New Mexico, 1:24 000 quadrangle (1952), north side of Santa Clara Canyon road, 6300 ft N. 10 W. of N.W. cor., sec. 20, T. 20 N., R. 6 E. Seven samples spanning 25 m.
2. Guaje Mountain, New Mexico, 1:24 000 quadrangle (1952), north side of Santa Clara Canyon Road, 11 100 ft N. 20 W. of N.W. cor., sec. 20, T. 20 N., R. 6 E. Seven samples spanning 18 m.
3. Cañones, New Mexico, 1:24 000 quadrangle (1953), 2000 ft N. 42 E. of BM 7909 on rim of Polvadera Mesa. Eight samples spanning 35 m.
4. Polvadera Peak, New Mexico, 1:24 000 quadrangle (1953), on E. side of road near Polvadera Sawmill Camp, 1000 ft S. 32 E. of BM 7976. Eight samples spanning 43 m.

W5. Polvadera Peak, New Mexico, 1:24 000 quadrangle (1953), 7600 ft N. 72 W. of Polvadera Peak VABM 11232, 9100 ft elevation. Seven samples spanning 20 m.

W6. Polvadera Peak, New Mexico, 1:24 000 quadrangle (1953), in bottom of Cañada del Ojitos, 5600 ft S. 77 W. of BM 8272. Eight samples spanning 30 m.

W7. Cañada, New Mexico, 1:24 000 quadrangle (1953), E. side of Bland Canyon Road, 1200 ft, S. 60 W. of N.W. cor., sec. 5, T. 17 N., R. 5 E. Eight samples spanning 31 m.

W8. Cañada, New Mexico, 1:24 000 quadrangle (1953), N.E. side of road near Rancho Cañada, on spur 1600 ft N. 16 E. of hill 6563. Nine samples spanning 45 m.

W9. Frijoles, New Mexico, 1:24 000 quadrangle (1953), on roadcut just N. of lookout tower top of St. Peters Dome. Eight samples spanning 41 m.

W10. Bland, New Mexico, 1:24 000 quadrangle (1953), N. side Hwy. 4, 600 ft N. 79 E. of BM 8812. Eight samples spanning 37 m.

W11. Polvadera Peak, New Mexico, 1:24 000 quadrangle (1953), E. side of Abiquiu Creek, 2100 ft N. 48 E. of hill 8879. Eight samples spanning 11 m.

W12. Grants, New Mexico, 1:24 000 quadrangle (1957), 2000 ft due W. of N.E. cor. of sec. 1, T. 11 N., R. 9 W. Eight samples spanning 1300 m. Geologic ref. [24].

W13. Jordan Valley, Oregon, Idaho, 1:250 000 quadrangle (1958), T. 33 S., R. 40 E., flow exposed at water level on S.E. shore of reservoir at dam on Crooked Creek 3.8 km S.W. of confluence of Crooked and Rattlesnake Creeks. Eight samples spanning 90 m. Between 4½-8 miles N.E. this flow is overlain by sediments that contain the Hemphillian Rome Local Fauna of mammals, birds, fish and mollusks. About 15 miles S.S.W. it overlies sediments that contain a Barstovian mammal fauna. It appears to be continuous with basalt flows 30 miles S.W. that overlie the Trout Creek Formation of Smith [26] which contains late Miocene flora and fauna [25, 27]. Sample from map unit Tb of ref. [18].

W14. Dayville, Oregon, 1:125 000 quadrangle (1932), sec. 27, T. 12 S., R. 25 E., approximately one-half mile north of Birch Creek School and one-fourth mile west of Birch Creek at elevation 3300 ft. Six samples spanning 47 m from a friable white rhyolite tuff 8-10 m thick has been reported by for a different outcrop Rattlesnake Formation relationship of our locality of Evernden et snake flora and fauna. W14, but there is in dence to determine wh the same cooling unit.

W15. Same locality as W: spanning 38 m from r lying W14.

W16. Burns, Oregon, 1: (1959), T. 20 S., R. 36 from Drinkwater Pass. ning 100 m. This rhyoli lowest member of the of Bowen et al., in S stratigraphically below na of Hemphillian age [: on sanidine previously same locality.

W17. Adel, Oregon, 1:250 00 T. 36 S., R. 40 E., 2.4 4525, 30 m east of Tw elevation 4800 ft. Ten 80 m. From map unit T: map unit (Ttr) is local beds of the Trout C: Smith [26] which conta cene Trout Creek flora of early and late (?) E The exact stratigraphic sample to the fossil-b known.

W18. Jordan Valley, Oregon, quadrangle (1958), T. 3 m east of ranch on Batt ples spanning 35 m. Fr [18]. At our sample loc overlies sediments that mammals and are thoug [25] to the Trout Creek F [26]. See notes for W17.

W19. Huntoon Valley, 1:62 000 quadrangle (19 Hwy. 31, 1300 ft N. 32 E. samples spanning 20 m W21.

W20. 1200 ft N. 40 W. of W19 tion.

W21. 200 ft N. 40 W. of W19 a

W22. Virginia City, Nevada, 1: (1950), E. side of Louset S. of N. boundary, sec. 2:

. 1000 ft S. 32 E.
s spanning 43 m.
Mexico, 1:24 000
N. 72 W. of Pol-
2, 9100 ft eleva-
ting 20 m.
Mexico, 1:24 000
om of Cañada del
f BM 8272. Eight

24 000 quadrangle
anyon Road, 1200
sec. 5, T. 17 N.,
nning 31 m.
24 000 quadrangle
near Rancho Cañ-
6 E. of hill 6563.
m.
24 000 quadrangle
. of lookout tower
. Eight samples

24 000 quadrangle
00 ft N. 79 E. of
spanning 37 m.
Mexico, 1:24 000
side of Abiquiu
f hill 8879. Eight

24 000 quadrangle
N.E. cor. of sec.
t samples span-
. [24].
Idaho. 1:250 000
S., R. 40 E., flow
on S.E. shore of
ked Creek 3.8 km
ooked and Rattle-
amples spanning
N.E. this flow is
that contain the
Fauna of mam-
ollusks. About 15
sediments that
mal fauna. It ap-
th basalt flows 30
the Trout Creek
hich contains late
[25, 27]. Sample
[18].
25 000 quadrangle
R. 25 E., approx-
th of Birch Creek
lle west of Birch
) ft. Six samples
iable white rhyo-

lite tuff 6-10 m thick. An age of 6.4 m.y. has been reported by Evernden et al. [17] for a different outcrop of rhyolite from the Rattlesnake Formation. We do not know the relationship of our sample locality to the locality of Evernden et al. or to the Rattlesnake flora and fauna. Unit W15 overlies W14, but there is insufficient field evidence to determine whether both are from the same cooling unit. Geologic ref. [19].

W15. Same locality as W14. Seven samples spanning 38 m from red welded tuff overlying W14.

W16. Burns, Oregon, 1:250 000 quadrangle (1959), T. 20 S., R. 36 E., 150 m N. 30 E. from Drinkwater Pass. Ten samples spanning 100 m. This rhyolite welded tuff is the lowest member of the Drewsey Formation of Bowen et al., in Shotwell [20], and is stratigraphically below the Drinkwater fauna of Hemphillian age [20]. Age of 8.9 m.y. on sanidine previously reported [17] from same locality.

W17. Adel, Oregon, 1:250 000 quadrangle (1958), T. 36 S., R. 40 E., 2.4 km south of Ranch 4525, 30 m east of Twelve Mile Creek at elevation 4800 ft. Ten samples spanning 80 m. From map unit Ttr of ref. [23]. This map unit (Ttr) is locally interbedded with beds of the Trout Creek Formation of Smith [26] which contains the upper Miocene Trout Creek flora [27] and mammals of early and late (?) Barstovian age [25]. The exact stratigraphic relationship of our sample to the fossil-bearing beds is not known.

W18. Jordan Valley, Oregon, Idaho, 1:250 000 quadrangle (1958), T. 37 S., R. 43 E., 100 m east of ranch on Battle Creek. Six samples spanning 35 m. From unit Ttr of ref. [18]. At our sample locality map unit Ttr overlies sediments that contain Barstovian mammals and are thought to be equivalent [25] to the Trout Creek Formation of Smith [26]. See notes for W17.

W19. Huntoon Valley, Nevada-California, 1:62 000 quadrangle (1958), 700 ft N.W. of Hwy. 31, 1300 ft N. 32 E. of BM 7401. Nine samples spanning 20 m. Underlies unit W21.

W20. 1200 ft N. 40 W. of W19 at 7720 ft elevation.

W21. 200 ft N. 40 W. of W19 at 7530 ft elevation.

W22. Virginia City, Nevada, 1:62 500 quadrangle (1950), E. side of Lousetown Creek, 500 ft S. of N. boundary, sec. 21, T. 18 N., R. 21 E. Second flow above creek. Six samples spanning 73 m. Units W23-W25 and W32 are all distinctive biotite-augite latite welded tuffs that may be part of the same eruptive sequence [21].

W23. Huntoon Valley, Nevada-California, 1:62 500 quadrangle (1958), 500 ft S. 30 W. of BM 7257, 30 ft N.W. of Hwy. 31.

W24. Bodie, California, 1:62 500 quadrangle (1958), SW¼ of SW¼ of sec. 24, T. 3 N., R. 26 E. Eight samples spanning 27 m.

W25. Bodie, California, 1:62 500 quadrangle (1958), in roadcut on Hwy. 395, 600 ft due S. of BM 7594. Nine samples spanning 30 m.

W26. Alturas, California, 1:62 500 quadrangle (1961), NW corner of SE¼, sec. 17, T. 42 N., R. 11 E., 30 m south of Hwy. 299 at elevation 4480 ft. Three samples spanning 12 m from upper cooling unit and seven samples spanning 57 m from underlying unit are all normal. Dated sample from lower unit. The Alturas Formation of Dorf [28] contains Hemphillian fauna and flora and has also yielded a single specimen of a Barstovian mammal but the stratigraphic control on these fossils is poor. Evernden et al. [17] obtained a K-Ar age of 8.1 m.y. from the Alturas Formation. The relationship of sample W26 to the fossil localities and to the unit dated by Evernden et al. is unknown.

W27. Blairsden, California, 1:62 500 quadrangle (1956), NE¼ of SE¼ of sec. 16 (two samples) and SW¼ of sec. 15, T. 23 N., R. 13 E (two samples).

W28. Milford, California, 1:62 500 quadrangle (1950), SE¼ of SW¼ of sec. 11, T. 27 N., R. 16 E., at VABM 6998. Ten samples spanning 15 m. This is the uppermost of a series of 12 lava flows, all of which are normally magnetized.

W29. Dardanelles Cone, California, 1:62 500 quadrangle (1956), 9200 ft elevation on S. ridge of Bald Peak. Two adjacent samples. This latite flow overlies W32, but is separated from it by a similar lava flow that is also normally magnetized. Geologic ref. [21].

W30. Markleville, California, 1:62 500 quadrangle (1956), sec. 16 (unsurveyed), T. 8 N., R. 20 E., N. 41 W. from Highland Peak at elevation 8100 ft. Nine samples spanning 45 m. Geologic ref. [21].

W31. Donner Pass, California, 1:62 500 quadrangle (1955), 1000 m east from NW cor.

of sec. 17, T. 17 N., R. 15 E., at elevation 7600 ft. Seven samples spanning 13 m. Geologic ref. [21].

W32. Same locality as W29, at elevation 8880 ft. Two samples 2 m apart. This distinctive welded tuff occupies the same stratigraphic position as, and may be identical to, welded tuffs that are also reversely magnetized and occur 21 km to the west at Whittaker Dardanelles and 49 km to the west at McKay's Point. At these two localities the tuff directly overlies a reversely magnetized massive latite flow on Table Mountain (sample W33) to the west [21]. The biotite-augite latite welded tuff at McKay's Point has been dated at 9.1 m.y. [21].

W33. Columbia, California, 1:62 500 quadrangle (1948), NE¼ of NE¼, sec. 30, T. 4 N., R. 15 E., on south flank of Rattlesnake Hill. Five samples spanning 7 m. Geologic ref. [21] (see notes for W32).

W34. Bishop, California, 1:62 500 quadrangle (1949), 750 m N. 33 W. from SE cor. of sec. 29, T. 7 S., R. 32 E. Eight samples spanning 80 m. Geologic ref. [22].

W35. Soldier Pass, California-Nevada, 1:62 500 quadrangle (1958), S. side of Route 63, SW¼ of the NW¼, sec. 19, T. 6 S., R. 37 E. Eight samples spanning 235 m. Overlies W36. Geologic ref. [22].

W36. Soldier Pass, California, 1:62 500 quadrangle (1958), SW¼ of SW¼ of sec. 24, T. 6 S., R. 36 E. Seven samples spanning 150 m. K-Ar sample from NE¼ of SW¼, T. 6 S., R. 37 E. Underlies W35. Geologic ref. [22].

Units A1-A17 are alkalic and tholeiitic basalts from the northwest coast of Nunivak Island in the Bering Sea. There is no previous geologic description of the volcanic rocks from Nunivak. All sample localities are sea cliff exposures, and the lateral spread of samples is about 10 m at each locality.

A1. Nunivak Island, 1:63 360 quadrangle sheet A7 (1952), Ikook Point at sea level. Overlain by unit A2. Five samples.

A2. Nunivak Island, 1:63 360 quadrangle sheet A7 (1952), Ikook Point, 20 m above unit A1. Four samples.

A3. Nunivak Island, 1:63 360 quadrangle sheet A7 (1952), Ikooksmiut, lower of two basalt flows exposed north of creek at this locality. Four samples.

A8. Nunivak Island, 1:63 360 quadrangle sheet A6 (1952), southeast end of Koweelik Bluff, 5.7 km west of BM 426 on Kimixthoruk Hill. Flow is 5 m above sea level. Four samples.

A11. Nunivak Island, 1:63 360 quadrangle sheet A6 (1952), Cape Algonquin. This is the second flow from the bottom of the sections exposed here. Underlies unit A12. Six samples.

A12. Nunivak Island, 1:63 360 quadrangle sheet A6 (1952), Cape Algonquin, stratigraphically above and 200 m northwest of unit A11. Four samples.

A15. Nunivak Island, 1:63 360 quadrangle sheet A6 (1952), Nash Harbor, 1.2 km north of VABM 158 at elevation 60 m. Six samples.

A17. Nunivak Island, 1:63 360 quadrangle sheet A6 (1952), Nash Harbor, capping sea cliff immediately north of VABM 158. Four samples.

ACKNOWLEDGEMENTS

We thank Edward Mankinen, Edward Roth, Richard Jones and Rene Bodmer for assistance with the magnetic measurements, and Wilfred Davis and Lois Schlocker for assistance with the argon and potassium measurements, respectively. C. A. Repenning contributed valuable information concerning relevant fossil localities. This work was partly supported by National Science Foundation Grant GF77, and part was done in the laboratory of Professor J. Verhoogen at the University of California, Berkeley, supported by National Science Foundation Grant GF74.

REFERENCES

[1] R. R. Doell, G. B. Dalrymple and A. Cox, Geomagnetic polarity epochs, Sierra Nevada data 3, J. Geophys. Res. 71 (1966) 531.

[2] R. R. Doell and G. B. Dalrymple, Geomagnetic polarity epochs, A new polarity event and the age of the Brunhes-Matuyama boundary, Science 152 (1966) 1060.

[3] F. H. Chamalaun and I. McDougall, Dating geomagnetic polarity epochs in Réunion, Nature 210 (1966) 1212.

[4] A. Cox, D. M. Hopkins and G. B. Dalrymple, Geomagnetic polarity epochs, Pribilof Islands, Alaska, Geol. Soc. Am. Bull. 77 (1966) 583.

[5] C. G. A. Harrison, The paleomagnetism of deep sea sediments, J. Geophys. Res. 71 (1966) 3033.

[6] N. D. Opdyke, B. Glass, J. D. Hays and J. Foster, Paleomagnetic study of Antarctic deep sea cores, Science 154 (1966) 349.

[7] F. J. Vine and D. H. Matthews, Magnetic anomalies over oceanic ridges, Nature 199 (1963) 947.

[8] F. J. Vine and J. T. Wilson, Magnetic anomalies over a young o Science 150 (19

[9] M. A. Lanphere interlaboratory potassium ana 3497.

[10] R. R. Doell and remanent magn ods in Paleom sterdam) in pre

[11] R. R. Doell and nent magnetism Survey Bull. 12

[12] R. R. Doell and field demagnet Paleomagnetism in press.

[13] A. Cox and G. B geomagnetic r potassium-arg press.

[14] E. L. Crow, F. tics manual (1960) 288 pp.

[15] C. S. Ross, R. the geology of New Mexico C (1961) 139.

[16] R. L. Smith an tion.

[17] J. F. Evernden James, Potas mammalian e Sci. 262 (1964

[18] G. W. Walker

over a young oceanic ridge off Vancouver Island. Science 150 (1965) 485.

[9] M. A. Lanphere and G. B. Dalrymple. P 207. An interlaboratory standard muscovite for argon and potassium analyses. J. Geophys. Res. 70 (1965) 3497.

[10] R. R. Doell and A. Cox. Measurement of natural remanent magnetization at the outcrop. In: Methods in Paleomagnetism (Elsevier Publ. Co., Amsterdam) in press.

[11] R. R. Doell and A. Cox. Measurement of the remanent magnetization of igneous rocks. U.S. Geol. Survey Bull. 1203-A (1965) 32 pp.

[12] R. R. Doell and A. Cox. Analysis of alternating-field demagnetization equipment. In: Methods in Paleomagnetism (Elsevier Publ. Co., Amsterdam) in press.

[13] A. Cox and G. B. Dalrymple. Statistical analysis of geomagnetic reversal data and the precision of potassium-argon dating. J. Geophys. Res., in press.

[14] E. L. Crow, F. A. Davis and M. W. Maxfield. Statistics manual (Dover Publ. Co., Inc., New York, 1960) 288 pp.

[15] C. S. Ross, R. L. Smith and R. A. Bailey. Outline of the geology of the Jemez Mountains, New Mexico. New Mexico Geol. Soc. 12th Field Conf. Guidebook (1961) 139.

[16] R. L. Smith and R. A. Bailey, private communication.

[17] J. F. Evernden, D. E. Savage, G. H. Curtis and G. T. James. Potassium-argon dates and the Cenozoic mammalian chronology of North America. Am. J. Sci. 262 (1964) 145.

[18] G. W. Walker and C. A. Repenning. Reconnaissance geologic map of the west half of the Jordon Valley quadrangle Malheur County, Oregon. Misc. Geol. Invest. Map I-457. U.S. Geol. Survey (1966).

[19] J. C. Merriam, C. Stock and C. L. Moody. The Pliocene Rattlesnake Formation and fauna of eastern Oregon, with notes on the geology of the Rattlesnake and Mascall deposits. Carnegie Inst. Washington Publ. 347 (1925) 43.

[20] J. A. Shotwell. The Juntura Basin. Studies in earth history and paleoecology. Trans. Am. Phil. Soc. 53, pt. 1 (1963) 77 pp.

[21] G. B. Dalrymple. Cenozoic chronology of the Sierra Nevada, California. California Univ. Publ. Geol. Sci. 47 (1964) 41 pp.

[22] G. B. Dalrymple. Potassium-argon dates of some Cenozoic volcanic rocks of the Sierra Nevada, California. Geol. Soc. Am. Bull. 74 (1963) 379.

[23] G. W. Walker and C. A. Repenning. Reconnaissance geologic map of the Adel quadrangle, Lake Harney and Malheur Counties, Oregon. Misc. Geol. Invest. Map I-446. U.S. Geol. Survey (1965).

[24] W. A. Bassett, P. F. Kerr, D. A. Schaeffer and R. W. Stoenner. Potassium-argon ages of volcanic rocks near Grants, New Mexico. Geol. Soc. Am. Bull. 74 (1963) 221.

[25] C. A. Repenning, personal communication (1966).

[26] W. D. Smith. Physical and economic geology of Oregon: The southeastern lake province. Oregon Univ. Commonwealth Rev. 8 (1926) 199.

[27] H. D. MacGinitie. The Trout Creek flora of southeastern Oregon. Carnegie Inst. Wash. Publ. 416 (1933) 21.

[28] E. Dorf. Pliocene floras of California. Carnegie Inst. Wash. Publ. 412 (1933) 1.